

Probabilistic short circuit analysis for VSC-HVDC systems in a dedicated cloud infrastructure

Guacira Costa de Oliveira* Renato Machado Monaro*
Denis Vinicius Coury*** Mario Oleskovicz*** Gilney Damm**

* *Polytechnic School, University of São Paulo, São Paulo, Brazil*

** *COSYS-LISIS, IFSTTAR, Université Gustave Eiffel, Marne-la-Vallée, France*

*** *São Carlos School of Engineering, University of São Paulo, São Paulo, Brazil*

Abstract: The main objective of this research is to carry out a probabilistic short circuit analysis, using the Monte Carlo Method (MCM), applied to Voltage Source Converter (VSC)-High Voltage Direct Current (HVDC) systems. The definition of stochastic parameters and a method to ensure statistical significance of the phenomenon under analysis are addressed. Due to the large number of cases involved in the MCM calculation, parallel programming hosted in a cloud computing environment was used. This procedure saves a considerable amount of time in the process, especially considering the time that would be spent using conventional transient programs. The result is the probabilistic density function that shows the probability of overcurrent and overvoltage magnitudes that the system may experience. This information is particularly important for component design, protection setting, life time expectancy assessment, grid stability and maintenance planning.

Keywords: Probabilistic Short Circuit; Monte Carlo; HVDC; Voltage Source Converter; PDF; CDF

1. INTRODUCTION

High Voltage Direct Current (HVDC) technology allows more efficient bulk power transfer over long distances. The main characteristics of HVDC transmission are flexibility of connections between systems with distinct operation frequencies, easy power flow control, enhancement of the Electric Power System (EPS) stability and reduction of losses in transmission lines (Meah and Ula, 2009, 2007). Most of the HVDC transmission lines in operation are based on Line Commuted Converter (LCC) technology (using thyristors). Recently, the Voltage Source Converter (VSC) in HVDC transmission systems has been discussed and used to improve their operational characteristics (Castro et al., 2015). One of the main advantages of a VSC-HVDC transmission system is the possibility of using multi-terminal transmission lines with different architectures, for example, connecting monopolar transmission lines to bipolar ones. Another potentiality of this technology is to integrate wind and solar generation plants into power systems using such technology (Yang et al., 2010). This is in tune with the new concept of smart grids, where smart microgrid concept-based Alternating Current (AC), Direct Current (DC), and hybrid architecture is gaining popularity due to the growing use of distributed renewable energy generation (Sahoo et al., 2021).

One important topic of study concerning VSC-HVDC systems is their transient behavior, especially during Short Circuit (SC) events (pole to ground and pole to pole faults) (Jiang and Gong, 2018). Thus, some research focusing on transient SC analysis has been carried out

(Lu and Sharma, 2008). Commonly, researchers use the Electromagnetic Transients Program (EMTP), based on Dommel's method, for this kind of analysis (Mauricio and Exposito, 2006; Yang, 2012; Wang et al., 2018). This choice is due to the lack of precise analytical methods to calculate DC short-circuit currents, despite the recent effort of some researchers to achieve this goal (Li et al., 2017; Kontos et al., 2014; Mourinho et al., 2015).

The EMTP was used for SC analysis (Sarajcev et al., 2016) and the recovery of a fault in a VSC-HVDC transmission line was studied by Yang et al. (2010). In reference (Mauricio and Exposito, 2006), stability analysis was compared with steady-state models. Additionally, in reference (Yang, 2012), severe SC conditions considering VSC systems was investigated. These papers discussed SC simulations, but did not address their probabilities of occurrence. The information about the probability of occurrence is paramount to ensure an economical design of the VSC-HVDC components such as: diodes, switches (GTO, Insulated Gate Bipolar Transistors (IGBTs) and others), reactors, capacitors and circuit breakers. Another outcome of this kind of analysis is the reliability improvement when over/under magnitude of voltage and current probability of occurrence are taken into consideration during the system design.

This paper proposes a method to calculate short circuit current and voltage profiles using Probabilistic Density Function (PDF) and Cumulative Distribution Function (CDF). This information is particularly important for component design, protection setting (Freitas et al., 2018),

life time expectancy assessment, grid stability and maintenance planning.

The technique often used for Probabilistic Short Circuit Analysis (PSCA) in EPSs is the Monte Carlo Method (MCM) (Kalos and Whitlock, 2008). Other methods rather than MCM, such as the Quasi-Monte Carlo and Latin Hypercube Sampling (Singhee and Rutenbar, 2010), can also be applied to PSCA. Most research using the MCM focuses on AC distribution, transmission and generation (Balouktsis et al., 1986; Gupta and Daratha, 2017). There is little published on the MCM in DC systems, especially VSC-HVDC transmission lines. The MCM requires a large number of simulations to ensure statistical significance of the phenomenon under analysis, which requires long computational time.

The specific focus of this study was PSCA using the MCM to explore all possible overcurrent and overvoltage values that circuit-breakers, lines, capacitors, IGBTs and diodes are exposed to. The MCM was implemented using the Message Passing Interface (MPI), parallel programming and was executed in a cloud computing environment. This saves a considerable amount of time in the process, especially considering the time spent in conventional transient programs.

2. PROPOSED METHOD

Numerical simulations have been used successfully to solve engineering problems, as well as to reproduce actual systems behavior. In order to carry out these tasks, building proper models that relate inputs and outputs are required. However, when the inputs of the models are non-deterministic, their implementation is not feasible. PSCA is one of these cases, in which its inputs are random, for example, fault location and fault resistance. This characteristic leads to non-deterministic outputs, such as transmission line fault currents. The aim of PSCA is to find PDF and CDF curves, showing the probability of a given current or voltage to occur.

In order to perform a PSCA based on MCM for HVDC-VSC transmission systems, the inputs (electrical components and related characteristics) and their probabilistic distributions need to be defined. This paper used the converter loading conditions (active and reactive power), a DC fault location, a DC fault resistance and a DC fault type as random inputs on the PSCA. For these variables, a sampling method was necessary to randomly select their values (within their probabilistic distribution).

For each case, an electromagnetic simulation was performed until a post fault steady state was reached. Afterwards, the maximum values of currents and voltages for each component under analysis were stored. This process was repeated until the PDF reached convergence, ensuring statistical relevance, resulting in voltage and current maximum values of PDF for each component under study.

In order to simulate all the SC cases necessary for the MCM, and reduce the amount of time to obtain the results, a dedicated cluster was used. The cluster was built in a cloud computing environment available at the University of São Paulo (USP) (STI, 2020). The virtual computing consisted of 6 virtual machines with 8 processors each, pro-

viding 64 computational nodes. One node was selected as the master node and it managed the slave nodes. The master node received the result of each simulation carried out in the slave nodes. The task management between nodes was performed using MPI (Indiana University, 2020). The flowchart in Figure 1 summarizes the steps of the proposed technique.

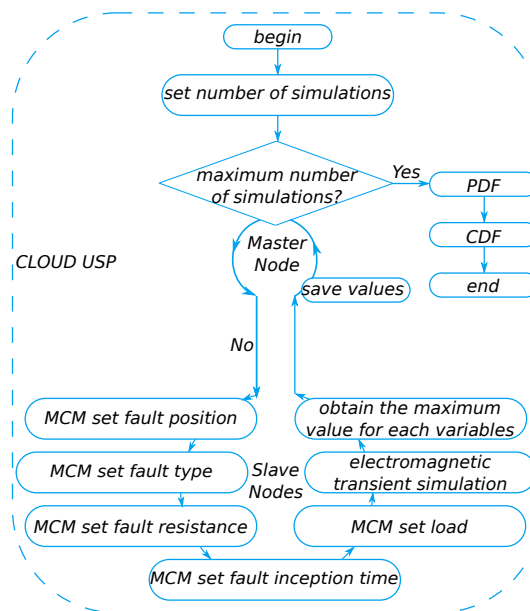


Figure 1. Proposed method flowchart

In the first step, the number of SCs to be simulated was provided to the master node by the user. Firstly, approximately a million SC cases were considered, and from this result, the Euclidean distance was used to observe the statistics convergence and to optimize the choice for the future simulations. Aiming to fulfill this topic, there is a discussion in Section 4.1, to detail the aspects and emphasize the importance of the number of SC cases to ensure the statistic relevance of the results.

In this research, all the SC cases considered were located on the transmission line, but the proposed method is able to deal with SC in different system components. The location, type, SC resistance and converters' load conditions were randomly defined by the MCM regarding their probability distribution function. The DC fault inception time was also defined randomly.

Having defined the SC parameters, a simulation task was dispatched to one of the slave nodes. The simulation duration was set to 200 ms. This value was used to ensure that the most relevant period of the transient (SC current and voltage peaks) was taken into consideration by the simulation. When a slave node finished a simulation task, it sent the relevant information (SC current and voltage maximum values) to the master node.

When all the SC cases were considered, the master node computed the PDF histogram and CDF graph from the data collected. The number of bins (bars) used to build the histograms was set according to the Square-Root Choice (Maciejewski, 2011). Section 4.2 describes this method.

3. THE ELECTRIC POWER SYSTEM STUDIED

The methodology proposed was applied to a symmetrical monopolar VSC-HVDC transmission system. However, the authors would like to emphasize that the proposed technique can be applied to other VSC-HVDC topologies. It consists of two 200 MVA VSC stations connected by a 100 kV transmission line, 75 km long. Each VSC station was simulated as a two-level converter with ideal switches. In order to save time concerning the number of SC cases needed according to Section 4.1, the EPS shown in Figure 2 was simulated in the cloud computing environment. As mentioned before, this procedure would save a considerable amount of time in the process, if implemented in a dedicated single-tenant cloud infrastructure.

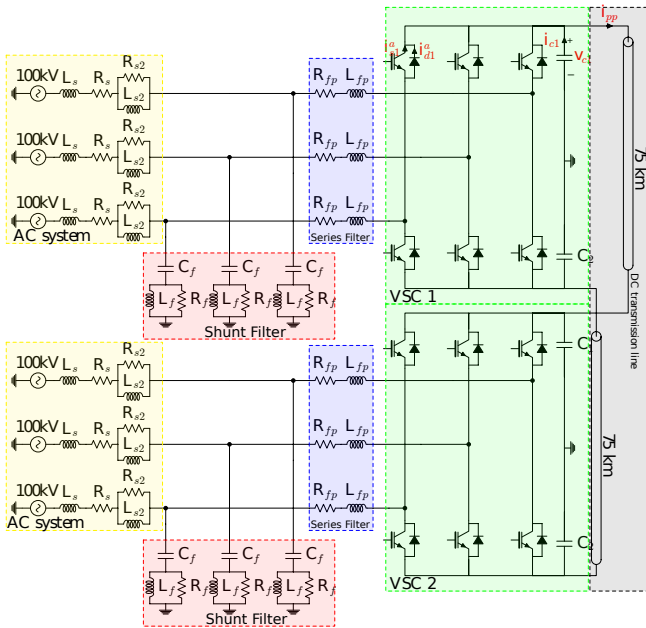


Figure 2. Representation of the EPS under study

Four sets of equipment can be observed in Figure 2: the AC, 100 kV 50 Hz, equivalent system with parameters $L_s = 23 \text{ mH}$, $R_s = 0.125 \Omega$, $L_{s2} = 5.86 \mu\text{H}$, and $R_{s2} = 2.6 \Omega$; the voltage harmonic filter (shunt filter) with $L_f = 0.8956 \text{ mH}$, $R_f = 11.25 \Omega$ and $C_f = 7.07 \mu\text{F}$; the current (series filter) with $L_{fp} = 23 \text{ mH}$ and $R_{fp} = 0.073 \Omega$; and the two-level converters with ideal switches and DC voltage ripple filter with $C = 280 \mu\text{F}$. The transmission line (75 km long) was simulated as a Bergeron model, without magnetic coupling. The line data are $L = 2.5 \frac{\text{mH}}{\text{km}}$, $R = 0.1088 \frac{\Omega}{\text{km}}$ and $C = 6.321 \frac{\text{nF}}{\text{km}}$. These distributed parameters were calculated from the physical parameters (conductor positions, tower dimensions and distance between towers) of a 110 kV transmission system (Ali, 2013), using the Line Constant routine from the Alternative Transients Program (ATP).

Six IGBTs were used for each VSC in the converter stations. Their self-commutation provided the independent active and reactive power control between the VSC terminals. For the VSC control, two different control strategies are commonly used: the direct control method and the vectorial control (Meshram and Borghate, 2012). The direct control method does not control the full range of currents

in VSC. For this reason, the vector control method was used to control both VSCs (Chen et al., 2014).

In this research, each station must control two variables, active and reactive power or DC voltage and reactive power. Figure 3 and Figure 4 show the control loops for active and reactive power. In Figure 3, PI_1 provides the control of the direct current component and PI_2 provides the activity power control. In Figure 4, PI_1 provides the control of the quadrature current component and PI_2 provides the reactive power control. Finally, Figure 5 presents the DC voltage control used.

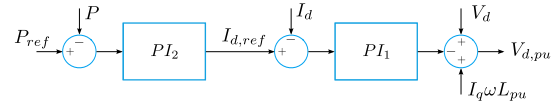


Figure 3. Converter control loops-active power control

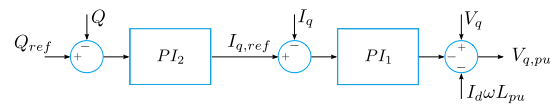


Figure 4. Converter control loops-reactive power control

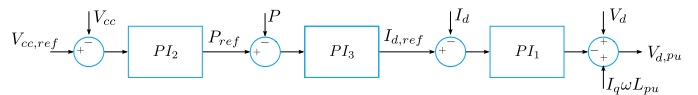


Figure 5. Converter control loops-DC voltage control

During the PSCA, active and reactive power references were defined randomly within operation limits. Therefore, it is important to check the settling time, the overshoot and to explore the capability curve of the converter to define proper operation limits. In order to validate the control settings (Figure 6), different reference values were set to the active and reactive power during the simulation time. The simulations showed that the overshoot occurs only for active power (oversignal amplitude $\cong 0.05 \text{ pu}$) and the margin of the capability curve was explored without causing over modulation.

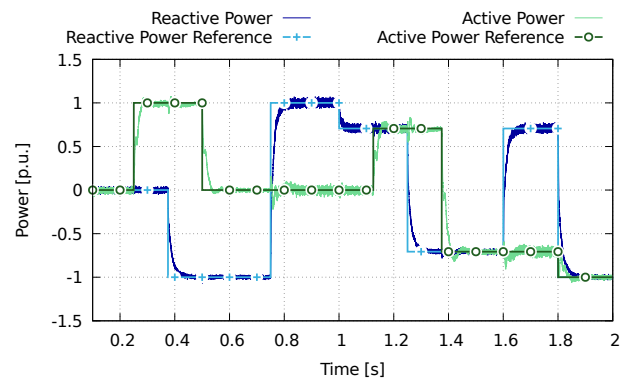


Figure 6. VSC control test

During fault events, the current in the IGBTs can easily exceed its supportable limit. In order to avoid damaging the switch, the converter control has a protection scheme that blocks the converter switches during over-current events. A typical value chosen to trigger this protection is 2 p.u. (Lu and Sharma, 2008).

Figure 7 depicts the IGBT protection used for this study: the I_{sp} is the positive DC cable current and the I_{sn} is the current from the negative DC cable. If I_{sp} or I_{sn} increases over the pickup value, a blocking signal is sent to the IGBT converter and a flip-flop device is used to keep the block state until reset is requested.

During the IGBT blockage, the currents flow through fly-wheel diodes. Therefore, the VSC becomes a non-controlled rectifier; see Figure 8 (Yang, 2012). Figure 9 shows a pole-ground fault inserted at $t = 0.15$ s. The positive DC line current and the IGBT block signal can be observed.

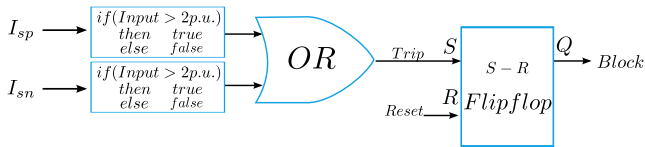


Figure 7. IGBT Over-current protection

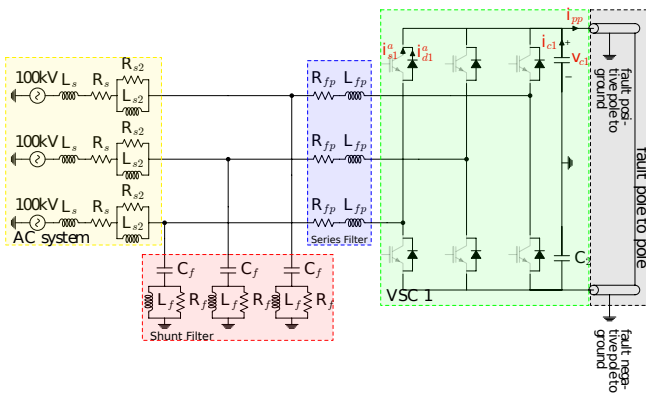


Figure 8. VSC circuit for non-controlled rectifier mode

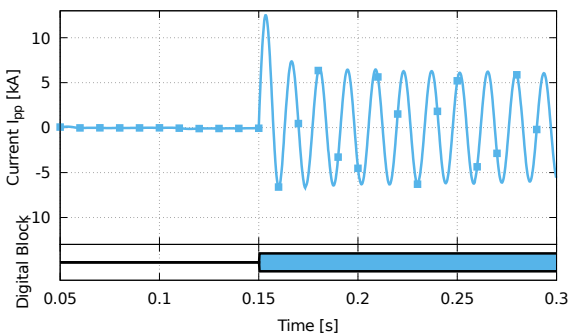


Figure 9. Pole-ground fault event and IGBT block signal

4. MONTE CARLO METHOD PARAMETERS

The aim of this study was to build short circuit current/voltage profiles using PSCA. The method was based on identifying the variables of the system model that presents random characteristics. Values generated by MCM was assigned to such variables. Considering this, the variable probability distribution was necessary to describe the actual behavior of fault events.

Fault type probability distribution of occurrence was considered 23 % for pole to pole faults, 38.5 % for positive pole to ground faults and 38.5 % for negative pole to ground faults. Given the lack of reliable data about fault event statistics in HVDC transmission systems, the values chosen for this study were inspired by the fault statistics observed for High Voltage Alternating Current (HVAC) transmission systems.

Distribution function $P(x)$, Equation (1), defines the probability of a short circuit to occur at a given transmission line location, x , where L is the transmission line length. It considers the uniform distribution, which implies that any position of the transmission line has equal probability ($\frac{1}{L}$) of fault occurrence (Balouktsis et al., 1986).

$$P(x) = \frac{1}{L} \quad (1)$$

The fault resistance probability, $P(R_{sc})$, Equation 2, is also defined using uniform distribution. This value was considered between a low value ($R_{Min} = 0 \Omega$) and a very high value ($R_{Max} = 100 \Omega$), which are typical values of SC resistance in a VSC-HVDC system (Bucher and Franck, 2013). Therefore, any value between R_{Min} and R_{Max} has equal probability to occur.

$$P(R_{sc}) = \frac{1}{R_{Max} - R_{Min}} \quad (2)$$

The system load was defined by the active and reactive power supplied to each converter. Their limits were defined by their capability curve. Hence, for each fault, active and reactive power was sorted by MCM, which means a different power flow through the transmission line and different reactive power exchange between converters and AC grids. The random selection of a load condition respected the converters' operating limits.

4.1 Random sampling generations and number of short circuit cases

PSCA is a method to describe the probability linked with over-currents/voltages created by fault events in the electrical system. Following this method, stochastic parameters representing different fault conditions were chosen. Various techniques can be used to generate these parameters. The most commonly used are the Pseudo-Random Generator (PRG) and Low-Discrepancy Sequences (LDS). PRG produces a random sampling while LDS creates parameters uniformly distributed. According to references (Keller et al., 2007) and (L'Ecuyer, 2017), many studies have used LDS due to the better convergence rate compared to the PRG. While the LDS convergence rate is $O(1/N)$ and the PRG is $O(1/\sqrt{N})$, where N is the number of samples.

In order to verify which method had better convergence considering the PSCA applied to HVDC-VSC, PRG and LDS were evaluated. To implement PRG, the plain Monte Carlo was used and, for LDS the Sobol and Niederreiter sequences (Lemieux, 2009) were implemented. The result of the PSCA was a histogram representing probability versus the overcurrent and overvoltage values, caused by fault events.

To evaluate the influence of the sampling method on PSCA convergence, twenty PDF histograms were carried out using PRG and the same number using LDS. Each histogram comprised a different number of cases; the smallest containing 100×10^3 cases and the largest containing 1000×10^3 cases of SC simulations. As a convergence metric, the Euclidean distance measure between consecutive histograms was used. Therefore, the Euclidean distance between histogram $\alpha = \alpha_1, \alpha_2, \dots, \alpha_n$ and histogram $\beta = \beta_1, \beta_2, \dots, \beta_n$, was obtained by Eq. (3).

$$d(\alpha, \beta) = \sqrt{(\alpha_1 - \beta_1)^2 + (\alpha_2 - \beta_2)^2 + \dots + (\alpha_n - \beta_n)^2} \quad (3)$$

Where α and β represent the values of bins for the two consecutive histograms. The distance reduction between two consecutive histograms indicates the process convergence.

Figure 10 shows the normalized distance for the PDF considered in the transmission line current on the positive pole by the plain Monte Carlo, Sobol and Niederreiter methods. The PDF histogram was built at every 5×10^3 simulations. For example, the first histogram used the first 100×10^5 samples (α); the second histogram was built using 150×10^3 samples (β) and so on. Through the normalized distance by the sampling methods, it can be concluded that the plain Monte Carlo method converged faster than the others.

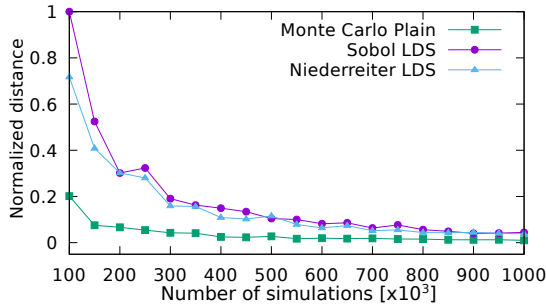


Figure 10. Euclidean distance between PDFs using Sobol, plain MCM and Neiderreiter methods

To ensure that other variables have the same convergence tendency using the plain Monte Carlo as the random sampling method, the normalized distance was performed (Figure 11) for i_{pp} , v_{c1} , i_{c1} and i_{s1}^a (see Figure 2). It can be observed that the other variables had the same convergence rate.

Another outcome of this analysis is the number of simulations required to ensure statistical relevance for PDF and CDF histograms. This can be inferred if the Euclidean distance does not decrease significantly when the simulation cases are increased between 150×10^3 to 300×10^3 resulting in a small variation of $\Delta 3\%$ (see detail in Figure 11). Therefore, the authors considered that 150×10^3 samples had shown the statistical significance and was used for the results presented in the next section.

4.2 Choice of a class interval

An important parameter to construct the histogram to represent the PDF is the number of bins. Each bin represents an interval of a current/voltage. As the number

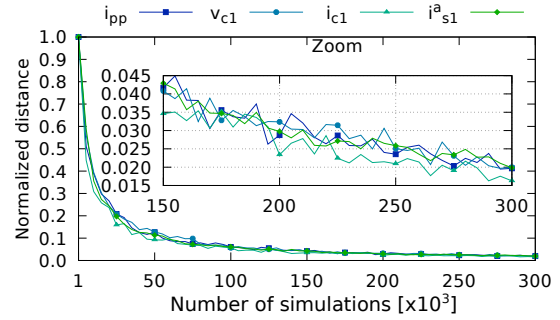


Figure 11. Euclidian distance by plain MCM for all the variables analyzed

of bins defines the data outline, some methods can be used to determine their proper size (Venables and Ripley, 2002). Equations (4) and (5) represent the Square-Root Choice Maciejewski (2011) and Sturges' Rule (Bowman and Robinson, 1987), respectively.

$$k = \sqrt{n} \quad (4)$$

$$k = 1 + \log_2 n \quad (5)$$

where k is the number of bins and n is the number of samples (SC simulations). Considering that 150×10^3 SC cases were simulated, Equations (4) and (5) result in 388 and 18 bins, respectively. The latter method results in a reduced number of bins that could lead to information loss. In order to be more representative, 388 bins were used in this research, which can be observed in the PDFs of Figures 12, 13, 14, 15 and 16.

5. PSCA RESULTS

This section shows the PSCA results for the proposed method applied to the EPS described in Section 3. Pole to pole, positive pole to ground and negative pole to ground faults were considered, totaling 150×10^3 faults.

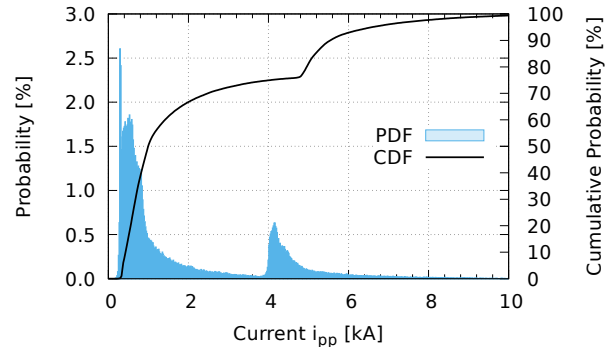


Figure 12. PDF and CDF for current i_{pp}

Figure 12 shows the PDF of maximum current values at the transmission line positive pole, i_{pp} . From the PDF curve, it can be observed that currents between 0.5 kA and 1 kA have the highest probability of occurrence followed by the current interval between 4 kA and 5 kA . It can also be observed that there are two regions (probability peaks) at the PDF curve. This phenomenon is associated with the fault type. Pole to ground faults have a greater chance of occurring than pole to pole faults. Conversely, pole to pole faults present higher current intensity. The CDF is also

shown in this figure, showing that fault currents higher than 6 kA have less than 7% probability of occurring. This result highlights that designing a component for the worst case (with low chance of occurrence) could lead to an oversized project. For example, selecting a circuit-breaker with disruptive capacity over 8 kA (it depends on the reliability required) may not be necessary for the system under analysis.

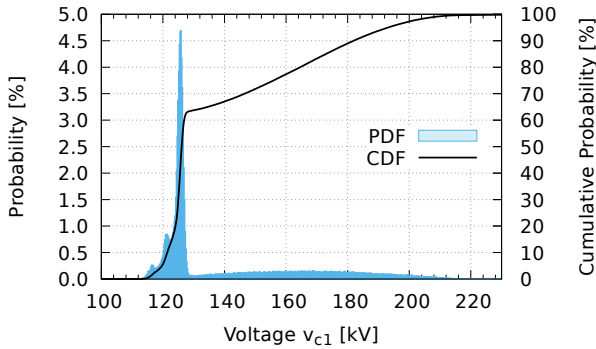


Figure 13. PDF and CDF for C_1 voltage

Figure 13 shows the PDF and CDF of voltage maximum values at the capacitor associated to the converter positive pole, v_{c1} . Considering the PDF curve, a peak of probability for the voltage range between 110 kV and 130 kV can be observed. CDF shows that this interval has up to 60% of chance of occurrence. The figure shows that the capacitor is exposed to over-voltages up to 200 kV, but with low probability (less than 5%).

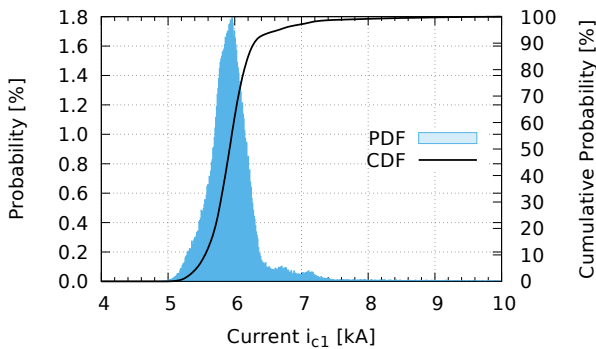


Figure 14. PDF and CDF for C_1 current

Besides over-voltage, another variable that can be observed in capacitors, especially during fault events, is its current. Extreme currents can damage the capacitor, disabling the converter operation. Figure 14 shows PDF and CDF curves for the current flowing through the capacitor connected to the converter positive pole. The highest probability of occurrence is restricted to the 5 kA to 7.5 kA interval, with a maximum probability at 6 kA. CDF shows that up to 98% of the currents are lower than 7.5 kA. This narrow range indicates that the choice of maximal current the capacitor has to support is critical for system's reliability.

Figure 15 shows the PDF and CDF for the current i_{d1}^a (see Figure 8) flowing through the fly-wheel diode $d1$ during fault events. From CDF, it can be observed that 60% of the currents are lower than 500 A. The PDF shows two

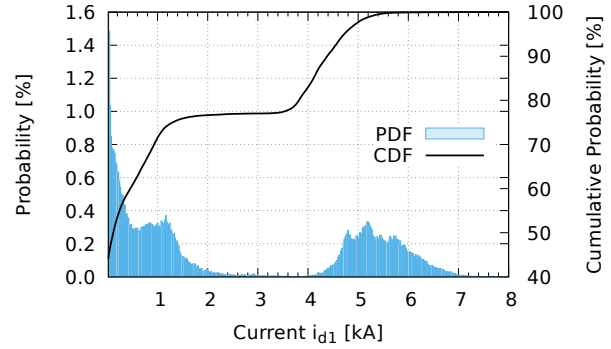


Figure 15. PDF and CDF for $d1$ Diode current i_{d1}^a

distinct regions: one from 0 kA to 3 kA and the other from 4 kA to 8 kA. The first is related to pole to ground faults and the second to pole-to-pole faults. It is worth noting that PDF indicates a high probability of currents lower than 200 A. The presence of two regions at PDF brings an important project aspect. If the design team selects a transmission layout that reduces the probability of pole-to-pole faults (this happens with cable transmission), diodes with lower maximum forward current rating can be used, reducing the project's overall cost.

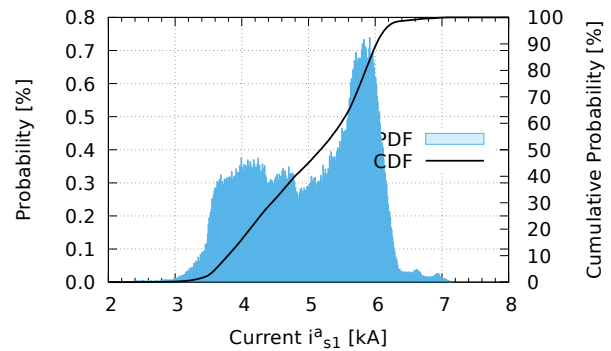


Figure 16. PDF and CDF for $s1$ IGBT current (i_{s1}^a)

Even with the protection that blocks IGBT operation for currents over 2 p.u. (4 kA in this simulation), the switches can experience higher SC currents for a short period of time, while the protection does not send the trip signal. This behavior can be observed in Figure 16, which shows PDF and CDF curves for the current i_{s1}^a of phase **A** up-arm switch. From the PDF, current probabilities are verified to range from 3 kA to 7 kA, with a peak near 6 kA. The CDF curve indicates that up to 99% of the SC currents observed are lower than 7 kA.

6. CONCLUSION

This paper proposed the use of parallel computing in a cloud environment in order to use the MCM to carry out a PSCA in a VSC-HVDC transmission system, as a way to minimize time spent in the process. The system under analysis had two-level VSC converters consisting of a monopolar symmetrical topology. The PSCA was used to build the PDF and CDF of the maximum current and voltage that the equipment was exposed to during fault events. Plenty of numerical simulations considering the system under analysis was presented and discussed in the

last section of the paper. This kind of information is crucial for maintenance planning, circuit design and protection algorithms.

The necessary number of simulations to ensure statistical relevance for AC systems by MCM was addressed by several papers, but no attention has been given to DC systems. This study gave special attention to DC systems and it proposed calculating the Euclidean distance between two consecutive PDFs as a criterion to determine the number of simulations to achieve statistical convergence. Besides, a comparison between three methods for sampling generation was presented, which was a key factor for PSCA. The results showed that the MCM plain sampling method presented faster convergence for a VSC-HVDC application. It was also shown that the Square-Root Choice method was adequate to define the histogram number of bins.

Finally, it must be highlighted that the authors consider that such a facility could be available to the Utility, implemented in a dedicated single-tenant cloud infrastructure, in a very near future.

ACKNOWLEDGMENTS

The authors acknowledge CAPES (Coordination for the Improvement of Higher Level Education Personnel) and Erasmus Mundus SMART2 (Project Reference: 552042-EM-1-2014-1-FR-ERA MUNDUS-EMA2) for the financial support. The authors also thank São Carlos School of Engineering and Polytechnic School both at the University of São Paulo, Brazil, and the Laboratoire des Signaux et Systèmes (L2S) at Supelec - Université Paris Saclay, France.

REFERENCES

- Ali, S.A. (2013). Modeling of power networks by ATP-Draw for harmonics propagation study. *Transactions on Electrical and Electronic Materials*, 14(6), 283–290.
- Balouktsis, A., Tsanakas, D., and Vachtsevanos, G. (1986). Probabilistic short-circuit analysis by Monte Carlo simulations and analytical methods. *IEEE Transactions on Power Systems*, 1(3), 135–140.
- Bowman, A.W. and Robinson, D.R. (1987). *Introduction to statistics*, volume 1. CRC Press.
- Bucher, M. and Franck, C. (2013). Contribution of fault current sources in multiterminal HVDC cable networks. *IEEE Transactions on Power Delivery*, 28(3), 1796–1803.
- Castro, L.M., Acha, E., and Fuerte-Esquivel, C.R. (2015). A novel VSC-HVDC link model for dynamic power system simulations. *Electric Power Systems Research*, 126(0), 111 – 120.
- Chen, Y., Damm, G., Benchaib, A., and Lamnabhi-Lagarigue, F. (2014). Multi-time-scale stability analysis and design conditions of a vsc terminal with dc voltage droop control for hvdc networks. In *53rd IEEE Conference on Decision and Control*, 3266–3271. IEEE.
- Freitas, G.D., Ismail, B., Bertinato, A., Raison, B., Niel, E., Poullain, S., and Luscan, B. (2018). Assessment methodology and performance indicators for hvdc grid protection strategies. *The Journal of Engineering*, 2018(15), 1002–1006. doi:10.1049/joe.2018.0185.
- Gupta, N. and Daratha, N. (2017). Probabilistic three-phase load flow for unbalanced electrical systems with wind farms. *International Journal of Electrical Power & Energy Systems*, 87, 154 – 165.
- Indiana University (2020). A high performance message passing library. Available in: <http://www.open-mpi.org/>. February the 22nd 2020.
- Jiang, B. and Gong, Y. (2018). Arm overcurrent analysis and calculation of mmc-hvdc system with dc-link pole-to-pole fault. *Electric Power Components and Systems*, 46, 1–10. doi:10.1080/15325008.2018.1432725.
- Kalos, M. and Whitlock, P. (2008). *Monte Carlo Methods, Volume 1: Basics*. Monte Carlo Methods. Wiley.
- Keller, A., Heinrich, S., and Niederreiter, H. (2007). *Monte Carlo and Quasi-Monte Carlo Methods 2006*. Springer Berlin Heidelberg.
- Kontos, E., Pinto, R.T., Rodrigues, S., and Bauer, P. (2014). Impact of hvdc transmission system topology on multiterminal dc network faults. *IEEE Transactions on Power Delivery*, 30(2), 844–852.
- Lemieux, C. (2009). *Monte Carlo and Quasi-Monte Carlo Sampling*. Springer Series in Statistics. Springer New York.
- Li, C., Zhao, C., Xu, J., Ji, Y., Zhang, F., and An, T. (2017). A pole-to-pole short-circuit fault current calculation method for dc grids. *IEEE Transactions on Power Systems*, 32(6), 4943–4953.
- Lu, B. and Sharma, S. (2008). A literature review of igt fault diagnostic and protection methods for power inverters. In *Industry Applications Society Annual Meeting, 2008. IAS '08*, 1–8. IEEE.
- L'Ecuyer, P. (2017). Randomized quasi-monte carlo: An introduction for practitioners. In *12th International Conference on Monte Carlo and Quasi-Monte Carlo Methods in Scientific Computing (MCQMC2016)*, Stanford, United States.
- Maciejewski, R. (2011). *Data Representations, Transformations, and Statistics for Visual Reasoning*. Synthesis digital library of engineering and computer science. Morgan & Claypool.
- Mauricio, J. and Exposito, A. (2006). Modeling and control of an HVDC-VSC transmission system. In *Transmission Distribution Conference and Exposition: Latin America, 2006. TDC '06.*, 1–6. IEEE/PES.
- Meah, K. and Ula, S. (2007). Comparative evaluation of HVDC and HVAC transmission systems. In *Power Engineering Society General Meeting*, 1–5. IEEE.
- Meah, K. and Ula, A.S. (2009). A self-coordinating adaptive control scheme for HVDC transmission systems. *Electric Power Systems Research*, 79(11), 1593 – 1603.
- Meshram, P.M. and Borghate, V.B. (2012). A voltage balancing method applied to direct control strategy of mmc-vsc-hvdc. In *9th International Conference on Electrical Engineering/Electronics, Computer, Telecommunications and Information Technology (ECTI-CON)*, 1–4.
- Mourinho, F.A., Motter, D., Vieira, J.C.M., Monaro, R.M., Le Blond, S.P., Min Zhang, and Weijia Yuan (2015). Modeling and analysis of superconducting fault current limiters applied in vsc-hvdc systems. In *2015 IEEE Power Energy Society General Meeting*, 1–5. IEEE.

- Sahoo, B., Routray, S.K., and Rout, P.K. (2021). Ac, dc, and hybrid control strategies for smart microgrid application: A review. *International Transactions on Electrical Energy Systems*, 31(1), e12683.
- Sarajcev, P., Vasilj, J., and Jakus, D. (2016). Method for estimating backflashover rates on hv transmission lines based on emtp-atp and curve of limiting parameters. *International Journal of Electrical Power & Energy Systems*, 78, 127 – 137. doi:<https://doi.org/10.1016/j.ijepes.2015.11.088>.
- Singhee, A. and Rutenbar, R. (2010). Why quasi-monte carlo is better than monte carlo or latin hypercube sampling for statistical circuit analysis. *IEEE Transactions on Computer-Aided Design of Integrated Circuits and Systems*, 29(11), 1763–1776.
- STI (2020). Cloud USP - Current Outlook. Available in: <http://www.sti.usp.br/?q=node/5370>.
- Venables, W. and Ripley, B. (2002). *Modern Applied Statistics with S*. Statistics and Computing. Springer.
- Wang, Y., Yang, B., Zuo, H., Liu, H., and Yan, H. (2018). A dc short-circuit fault ride through strategy of mmc-hvdc based on the cascaded star converter. *Energies*, 11, 2079. doi:10.3390/en11082079.
- Yang, J., Zheng, J., Tang, G., and He, Z. (2010). Characteristics and recovery performance of VSC-HVDC dc transmission line fault. In *Power and Energy Engineering Conference (APPEEC), 2010 Asia-Pacific*, 1–4.
- Yang, J. (2012). Short-circuit and ground fault analyses and location in VSC-based DC network cables. *IEEE Transactions on Industrial Electronics*, 59, 11.